

# Influence of Gravity on Inorganic Liquid Crystal



Zengzi Wang, Yun Chen, Dejun Sun, Shenghua Xu, Zhiwei Sun, Ding Lan and Yuren Wang

**Abstract** This chapter introduced the history of inorganic liquid crystals, and impact of gravity on phase transition was also discussed in detail. Inorganic liquid crystals are found to have different shapes including thread-like, rod-like or plate-like. They combine the good flowability and electrical properties of inorganic compounds, along with the superior thermal stability with low cost. However, for large size and weak particle–particle interactions, gravity can significantly influence the phase behavior of inorganic colloidal particles and liquid crystal phase transition. To rule out the impact of gravity, inorganic liquid crystal transition under microgravity will be a promising research aspect in future.

**Keywords** Microgravity · Inorganic liquid crystal · Polydispersity · Non-spherical particles · Dispersion

## 1 Introduction of Typical Inorganic Liquid Crystals

The liquid crystals have been investigated for over one hundred years, most of them are organic liquid crystals. In recent years, some researches on organic metal liquid crystals were reported [1]. However, real inorganic liquid crystals were still rare for the reasons listed below [2]: first, the building blocks must be highly anisotropic to form liquid crystal, while few inorganic compound can meet this standard; second, high melting point of inorganic compounds make it impossible to maintain anisotropic during the heating, and thus the thermotropic liquid crystals cannot be obtained. Another method to prepare inorganic liquid crystal is dissolving

---

Z. Wang · Y. Chen · D. Sun (✉)

Key Laboratory of Colloid and Interface Chemistry, Ministry of Education, Shandong University, Jinan 250100, Shandong, People's Republic of China  
e-mail: [djsun@sdu.edu.cn](mailto:djsun@sdu.edu.cn)

S. Xu · Z. Sun · D. Lan · Y. Wang

Key Laboratory of Microgravity (National Microgravity Laboratory), Institute of Mechanics, Chinese Academy of Sciences, No. 15 Beisihuanxi Road, Haidian District, Beijing 100190, China

© Science Press and Springer Nature Singapore Pte Ltd. 2019

151

W. R. Hu and Q. Kang (eds.), *Physical Science Under Microgravity: Experiments on Board the SJ-10 Recoverable Satellite*, Research for Development,  
[https://doi.org/10.1007/978-981-13-1340-0\\_7](https://doi.org/10.1007/978-981-13-1340-0_7)

or dispersing anisotropic inorganic compounds in the solvents to prepare lyotropic liquid crystal. Nevertheless, low dimensional (1D or 2D) inorganic compounds with solubility in water or other solvents were rarely reported. It is of high necessity to investigate the solubility of these inorganic compounds, the interaction between compounds and solvents, and the properties of dispersions. In addition, the preparation of organic liquid crystal is much easier than inorganic liquid crystal.

Despite of the difficulties in finding and investigating inorganic liquid crystals, some progresses have been achieved in decades. Freundlich [3] firstly found that  $V_2O_5$  sols can exhibit orientation order under electric field, magnetic field or flow. The orientation of long axes was in the same direction of electric field, magnetic field or flow. Once the orientation-inducing action was removed, the sols returned to their initial optically isotropic state. Zocher [4] further investigated the inorganic sols with induced optical anisotropy, especially for  $V_2O_5$ . They proved that the newly prepared  $V_2O_5$  sol will not exhibit induced birefringence. The birefringence will be enhanced with increasing ageing time. However, Zocher and Török [5] believe that  $V_2O_5$  sols should be regarded as “phase of a higher order” or “super phases” rather than lyotropic liquid crystals. Now it is clear that “super phases” are the same as thermotropic or lyotropic liquid crystals. The difference between  $V_2O_5$  sol and conventional liquid crystal can be attributed to the nematic phase formed by rod like particles. Similar anisotropic bentonite sols were also reported by Langmuir [6].

The size of inorganic liquid crystal building blocks varies from 10 to 1000 nm, which can be regarded as colloids. They are found to have different shapes including thread-like, rod-like or plate-like. The inorganic lyotropic liquid crystals combine the flowability and anisotropic of liquid crystals with the electrical properties (including high conductivity or magnetism etc.) of inorganic compounds, and they have thermal stability superior to that of organic ones. In addition, many of these inorganic liquid crystals are prepared by natural minerals with low cost. These advantages of inorganic liquid crystals promise their potential application in future works, and in recent years they have been focused by researchers again.

## 1.1 Rod-like Inorganic Liquid Crystals

Two kinds of liquid crystal phases can be formed by rod-like inorganic particles: nematic phase and smectic phase. The mechanism of liquid crystals formed by rod-like particle suspensions can be explained by Onsager's theory.

Vanadium pentoxide ( $V_2O_5$ ) suspension (Fig. 1) was the firstly reported inorganic lyotropic liquid crystals, nematic phases could be observed in this system. The real morphology of  $V_2O_5$  particles is ribbon-like (Fig. 1b). In general,  $V_2O_5$  particle have a thickness of 1 nm, a width of 25 nm, and a length up to thousand nanometers, which can be adjusted by preparation method and time. Researchers often regard them as rod-like to avoid more calculations. The phase behavior of suspension depends on the volume fraction ( $\Phi$ ) rather than temperature [7–9]. With the increasing concentration (critical  $\Phi = 0.7$  vol%), transition from isotropic phase (I) to nematic phase (N) can

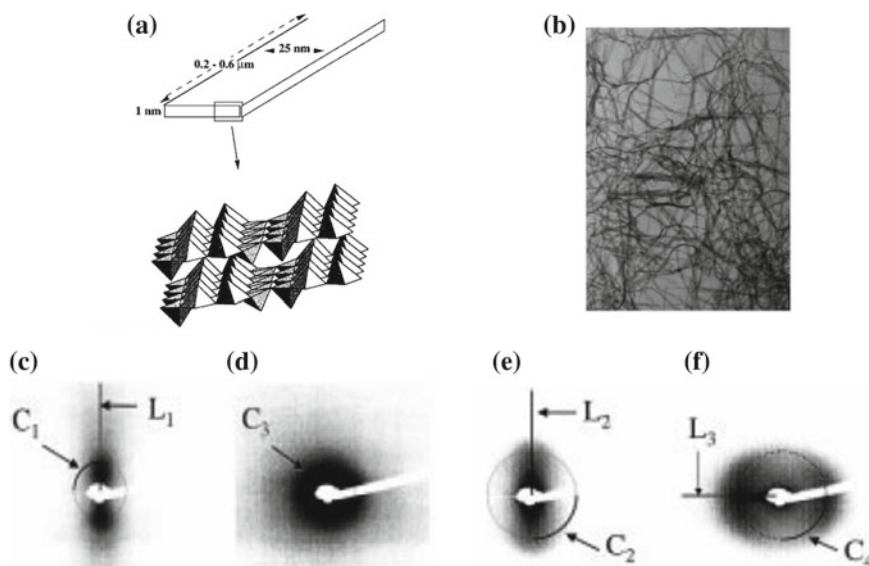


**Fig. 1** **a** Structure of crystalline  $V_2O_5$ . **b** SEM micrograph of  $V_2O_5$ . **c** and **d** 2-D scattering patterns obtained at the 2 vol% sample, can be regarded as  $N_u$ ; **e** and **f** at the 5 vol% sample, can be regarded as  $N_b$ . Reprinted with permission from (Langmuir **2000**, 16, (12), 5295–5303). Copyright (2000) American Chemical Society

be observed in the system. The primary phase transition can be explained by Onsager model; when  $\Phi$  comes to 1.2 vol%, the sol–gel transition is observed in the system; with higher concentration ( $\Phi = 5.0$  vol%), the system turns from uniaxial nematic ( $N_u$ ) to biaxial nematic ( $N_b$ ). The thermo-dynamic and fluid-dynamic properties can be explained by hard-core models. The  $V_2O_5$  sol and gel show long range order and typical nematic textures. The sol–gel transition concentration depends on ionic strength of the system.

Magnetic field and electric field can influence the structure of tactoids. Commeinhes et al. [10] investigated the impact of magnetic field on  $V_2O_5$  nematic sols. The application of magnetic field removes the topological defects and produces completely aligned nematic single domain. The orientation time of particles depends on the magnetic intensity and suspension concentration. For example, orientation time for 0.7 vol% suspension in 0.3 T and 1 T magnetic field is 2 h and 5 min, respectively. A sudden change in magnetic field orientation leads to transient hydrodynamic instability of samples.

One of main application of organic liquid crystal is panel display. However, compared to thermotropic liquid crystals, electro-optic effect is hard to be observed in the inorganic lyotropic liquid crystals, for the conductivity of water and the electrochemical reaction in aqueous systems. According to Lamarque-Forget et al. [11],  $V_2O_5$  suspension also shows electro-optic effect under the AC field. Under effective

voltages of 10 V, the response times are in the range of one second, making them suitable for slow display applications.

Researchers have made much progress in the application of  $V_2O_5$ . Desvaux et al. [12] applied the  $V_2O_5$  suspension as anisotropic medium in the NMR of biomacromolecules. Camerel et al. [13] used  $V_2O_5$  liquid crystals as templates to synthesize single-domain mesostructured inorganic composites. Several advantages including the low cost of  $V_2O_5$  suspensions, the low magnetic field needed, and the simplicity of the synthesis facilitates many industrial applications.

The liquid crystal properties of boehmite ( $\gamma$ -AlOOH) needle-like crystallite were firstly reported by Zocher, and were investigated thoroughly by Buining et al. [14]. They prepared boehmite rod-like particles with diameter of 8 nm, length of 130 nm and 280 nm. I-N phase separation can be observed in long rods (280 nm) suspension ( $\Phi = 0.1$  wt%) at low ionic strength after standing for one month. At boehmite concentration above 0.67 wt% or higher, permanently-birefringent monophasic dispersion will be obtained. For short rods (130 nm) suspension, liquid crystal phase can be observed with increasing concentration, while no phase separation appeared. Untreated boehmite particles are positively charged. To discuss their phase behavior, it is necessary to combine Onsager's model and DLVO theory together. Increasing ionic strength lead to the formation of gel network in the system and the phase separation will be influenced. The boehmite particles were also grafted by polyisobutene and dispersed in cyclohexane to obtain sterically stable suspensions [15]. The polymers prevent the contact of particles and weaken electrostatic repulsions and Van der Waals interaction. Only excluded volume effect and steric repulsion exist in the system, which can be explained by Onsager's theory.

Goethites ( $\alpha$ -FeOOH) are widespread iron oxide and mainly served as industrial pigments. Davidson et al. [16] researched the liquid crystals in polydisperse goethite particles suspension. Unexpected physical properties were observed in this system. Without magnetic field, I/N phase separation occurs with the concentration increased to critical value, and the border of two phase is clear. Nematic phase is clearly observed and further proved by SAXS. In magnetic field, the particles orient along the field direction at magnetic intensities smaller than 350 mT, but they reorient perpendicular to the field beyond 350 mT. This outstanding behavior was also observed in isotropic phase, which has very strong magnetic-field induced birefringence. For bulk goethite, it is a typical antiferromagnetic material. While nanorod goethite is an unusual magnetic behavior and carries a small magnetic moment, which can be explained by uncompensated surface spins.

Rod-like akaganeite ( $\beta$ -FeOOH) nanoparticles can form smectic phase in aqueous dispersions. Zocher and Birstein [17] found a stable and ordered structure in the sol sediments of  $\beta$ -FeOOH, called "Schiller layers", which exhibits brilliant interference colors. The thickness of ordered layer structure is similar to wavelength of visible light. The interference colors can be explained by Bragg reflection. Using atomic force microscopy to observe the akaganeite liquid crystal, Maeda and Maeda [18] found there are several kinds of smectic phase. The particles show different orientation in different areas. In the iridescent regions, the akaganeite crystals are

standing upright at a tilt (with respect to the plane of the smectic layer) and form approximately a square lattice. In contrast, in noniridescent regions, the crystals lie parallel or randomly oriented to each other.

## 1.2 Plate-like Inorganic Liquid Crystals

Langmuir [6] observed isotropic phase and birefringence phase, in the separated clay suspension after standing for hundreds of hours. With the help of crossed polarizer, Emerson [19] found band formation in the clay systems similar to that of Tobacco Mosaic Virus systems, and thus indicating clay suspensions are also able to form liquid crystals. The clay systems have been widely investigated, especially for montmorillonite and laponite. Montmorillonite is one kind of expanding 2:1 layered clay (two silica-oxygen octahedron and one aluminum-oxygen tetrahedron) with 1 nm thickness after being exfoliated successfully. The diameter of montmorillonite ranges from 50 to 500 nm with high aspect ratios. Laponite is one kind of montmorillonite. The diameter of monodisperse laponite particles is 25 nm and the thickness is 1 nm. Montmorillonite systems are typical charged plate-like liquid crystal systems, their phase behavior can be explained by Onsager and DLVO theories. Using polarization microscopy to observe montmorillonite and laponite suspensions, threaded textures of nematic liquid crystal are obvious. The properties of clay suspensions depend on volume fraction of clay and ionic strength [20]. For clay suspensions, the sol/gel transition concentration is lower than I/N transition concentration. Under low ionic strength, with increasing clay concentration, suspensions turn from isotropic sol to isotropic gel, and finally form nematic gel. The network structure of gel hinders the macroscopic phase separation of birefringence phase and isotropic phase, and thus nematic phase will not form. Furthermore, the aspect ratio of clay particles is low. The competition of excluded volume effect and electrostatic interaction make the I/N phase unable to co-exist in clay suspension. Temperature, electric field and magnetic field do not influence the orientation of nematic phase gel [21, 22]. For clay suspensions, increasing ionic strength and suppressing double layer make it easier to gel and I/N phase separation will take place, thus make the nematic phase stable (Fig. 2e, f). However, further increasing ionic strength will totally screen the electrostatic repulsion and lead to flocculation of suspensions.

Onsager's theory and computer simulations illustrated the presence of I-N phase separation in the plate-like particle suspension. van der Kooij et al. [23] found a new model system and proved this theory. The  $\text{Al}(\text{OH})_3$  plate-like hexagonal particles were grafted by polyisobutene ( $M_n \sim 1000$ ) and dispersed in cyclohexane or toluene. Only short range repulsion exists in this sterically stable system. At low concentration, I-N phase separation take place; with increasing concentration, the ratio of nematic phase increase gradually to 100%, along with increasing thermal stability of liquid crystal. The polydispersity of particles broaden the I/N biphasic region. and the width of biphasic region is proportional to the polydispersity of particles.

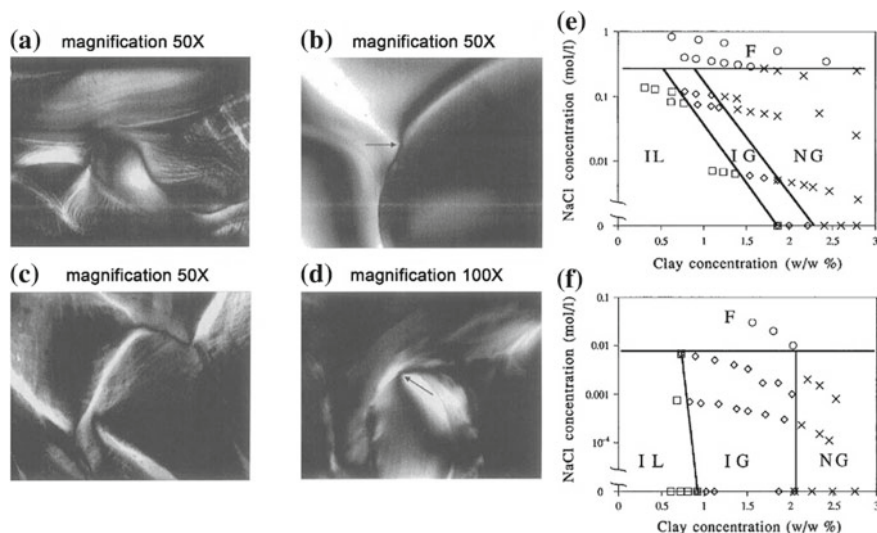
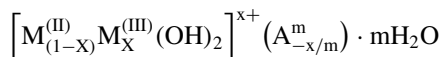


**Fig. 2** **a** Nematic threaded texture of a bentonite suspension. **b** Detail of a  $1/2$  disclination line (arrow) in a bentonite suspension. **c** Nematic threaded texture of a laponite suspension. **d** Detail of a  $1/2$  disclination line (arrow) in a laponite suspension. **e** Phase diagram of the bentonite suspensions versus clay and NaCl concentrations. ( $\circ$ , F) Flocculated samples; ( $\square$ , IL) isotropic liquid samples ( $\diamond$ , IG) isotropic gel samples; ( $\times$ , NG) nematic gel. **f** Phase diagram of the laponite suspensions versus clay and NaCl concentrations. Reprinted with permission from (The Journal of Physical Chemistry **1996**, 100, (26), 11139–11143). Copyright (1996) American Chemical Society

$\text{Al}_{13}$ -ions ( $\text{Al}_{13}\text{O}_4(\text{OH})_{24}(\text{H}_2\text{O})_{12}^{7+}$ ) were adsorbed to  $\gamma\text{-Al}(\text{OH})_3$  to prepare charged particles. Van der Beek and Lekkerkerker [24] used this system to investigate the phase behavior of charged plate-like particles.  $\text{Al}_{13}$ -ions increase the surface charge of  $\text{Al}(\text{OH})_3$  and thus enhancing the colloidal stability. The critical concentration at gel become higher than that of liquid phase transition, the gel structure will no more influence the liquid crystal phase in the system. According to the literature, with increasing particle concentration, I/N phase separation will be observed prior to the gel. The volume fraction of nematic phase decreases with increasing ionic strength and decreasing particle concentration.

Layered double hydroxides (abbreviate for LDHs) [25] are hybrid metal hydroxides composed by divalent and trivalent metal ions, which have hydroxide layered crystalline structure. LDHs particles are always positively charged for isomorphous replacement, the anions will adsorb between the layers to equilibrate charges. The interlayer spacing varies with different anions, and LDHs are regarded as anion clays; In contrast, montmorillonite clays are always negatively charged, which can be called cation clays. The anion clays rarely exist in nature but are easy to be synthesized in laboratory. The unique structure and electrical properties of LDHs endows their wide potential applications in catalyst, catalyst carrier, ion exchanger and pharmaceuticals.

The component of LDHs can be illustrate by following formula:



$M^{(II)}$  is divalent metal cations (e.g.  $\text{Mg}^{2+}$ ,  $\text{Mn}^{2+}$ ,  $\text{Fe}^{2+}$ ,  $\text{Ni}^{2+}$ ,  $\text{Cu}^{2+}$ ,  $\text{Zn}^{2+}$ ,  $\text{Ca}^{2+}$ ),  $M^{(III)}$  is trivalent metal cation (e.g.  $\text{Al}^{3+}$ ,  $\text{Cr}^{3+}$ ,  $\text{Mn}^{3+}$ ,  $\text{Fe}^{3+}$ ,  $\text{Co}^{3+}$ ,  $\text{Ni}^{3+}$ ,  $\text{La}^{3+}$ ); A is anion with n valence number (e.g.  $\text{Cl}^-$ ,  $\text{OH}^-$ ,  $\text{NO}_3^-$ ,  $\text{CO}_3^{2-}$ ,  $\text{SO}_4^{2-}$ ), x is the number of trivalent metal ions, m is the number of bonded water.

LDHs can be structurally characterized as containing brucite ( $\text{Mg}(\text{OH})_2$ ) like layers [26], in which some divalent metal cations have been substituted by trivalent ions to form positively charged sheets. The metal cations occupy the centers of octahedra whose vertices contain hydroxide ion. These octahedra are connected to each other by edge sharing to form an infinite sheet. The cationic charge created in the layers is compensated by the presence of hydrated anions between the stacked sheets. These anions can be replaced by other anions.

Stupp and Braun [27] reported the effects of Ca–Al–LDHs on molecular manipulation of microstructures. Using organic molecules modified LDHs can synthesize monodisperse rosettes organic-inorganic composite. The molar ratio of Ca–Al in the composite is the same as in the LDHs, the mass proportion of organic molecules is 20%. The amount of organic molecules intercalated into the layers depend on the structures of LDHs. Removing the organic molecules by heating will not change the rosettes structure of composite. The modification of organic molecules significantly enhanced the mechanical properties of LDHs.

Sun et al. [28] investigated the LDHs lyotropic liquid crystals (Fig. 3). With the LDHs dispersion concentration increasing (>16 wt%), birefringent nematic phase initially forms; when the concentration came to 34 wt%, stable nematic phase formed and no phase separation is observed; under the polarization microscope, the dispersion at 18 wt% initially shows a band-type texture caused by shear or flow, then nematic droplets appear and finally develop into a threaded texture, typical of nematic phase. LDHs can serve as better model systems to investigate phase transitions in electrostatically stabilized platelike colloids.

Graphene oxide (GO) is one typical kind of 2D particles, which can be prepared by oxidation of graphite. Plenty of oxygenated functional groups (hydroxyl, epoxy, ketone and carboxyl) are connected both to the basal plane and edge, and thus render the GO particles to hydrophilic. Intrinsic anisotropy properties and high aspect ratio of GO makes it a good 2D particle to form liquid crystals in water, DMF or NMP dispersions.

Xu and Gao [29], Kim et al. [30] and other groups [31] reported the liquid crystallinity of graphene oxide aqueous dispersions almost at the same time (Fig. 4). With the increasing concentration (0.05–0.5 vol%), the volume fraction of nematic phase increases, and reaches maximum value at 0.4 vol% (Fig. 4b). Under the crossed polarizer, typical nematic schlieren texture can be observed at the bottom phase. Polarization microscopy observation proves the existence of birefringent texture of the graphene oxide liquid crystals, which exhibit a high density of  $\pm 1/2$  disclinations (Fig. 4d). As the concentration further increase, regular lamellar phase can be observed.

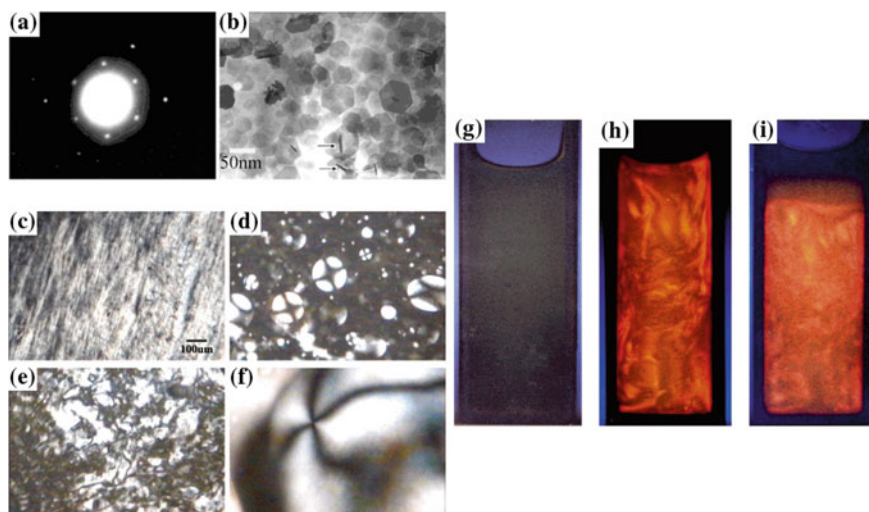


**Fig. 3** Nematic phase formed in LDHs aqueous dispersion. **a** Electron diffraction pattern and **b** TEM images of Mg/Al LDH particles. Rare (see arrow) edges of the particles can be seen. **c** 18% (w/w) dispersion. **d** Samples observed after 7 days and **e** 17 days. **f** Schlieren texture with a point defect surrounded by four dark brushes of 22% (w/w) dispersion. **g** Isotropic phase of the 16% (w/w) dispersion. **h** Birefringent nematic phase of the 27% (w/w) dispersion. **i** Isotropic-nematic phase separation of the 27% (w/w) dispersion, as observed 7 days after dilution. Reprinted with permission from (Chemistry of materials **2003**, 15, (17), 3240–3241). Copyright (2003) American Chemical Society

As GO are one atom thick, its aspect ratio is usually very large (700–2600). High aspect ratio leads to much lower isotropic-nematic transition concentration. GO aqueous dispersion can be rather stable for high absolute value of zeta potential. However, adding salts or changing pH will destroy its the liquid crystal structure. Increasing salt concentration will screen the electrostatic repulsion, and absolute value of zeta potential will be decreased. Changing pH to acid will protonated the –COOH groups on the GO [32], leading to reduced hydrophilicity and destabilize the liquid crystal.

Several researches were also performed on liquid crystals formed by chemically functionalized graphene. For reduced GO (RGO), decreased hydrophilicity makes it impossible to form liquid crystal in water. Poulin et al. [33] used bile salts as surfactants to stabilize RGO aqueous dispersion. An isotropic-nematic transition is observed as concentration of RGO increased. Corresponding SAXS 2D pattern also verified the formation of nematic ordering in RGO LC. Physical adsorbed or chemical grafted GO or RGO can also form liquid crystals. For example, Polyvinyl alcohol (PVA) wrapped RGO can be well dispersed in water and form LCs similar to GO [34]. Hyperbranched polyglycerol (HPG) enveloped GO and RGO show good solubility in NMP, and thus the nematic and lamellar phases are observed in the dispersion [35].

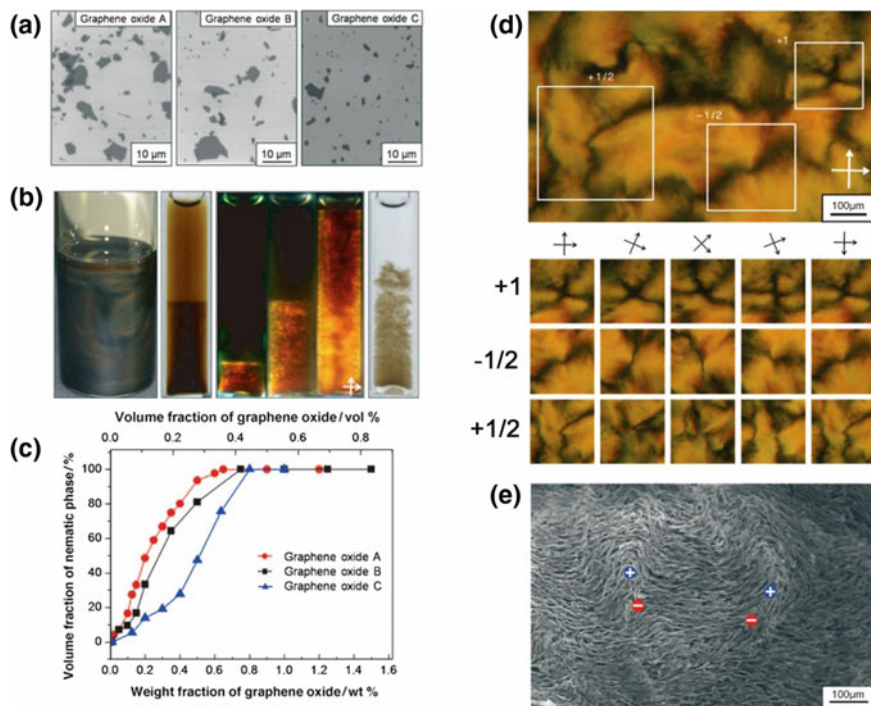


**Fig. 4** **a** SEM images of graphene oxide platelets exfoliated from various graphite sources. **b** Left to right: 0.5 wt% graphene oxide dispersion; phase-separated 0.2 wt% dispersion three weeks after preparation; phase-separated dispersions (0.05, 0.2, 0.5 wt%) located between crossed polarizers; coagulated 0.01 wt% dispersion upon adding 50 mM NaCl. **c** Nematic phase volume fraction versus graphene oxide concentration. **d** Typical nematic schlieren texture of a 0.3 wt% dispersion with  $\pm 1/2$  disclinations and  $+1$  disclination. **e** SEM image of GO liquid crystal in freeze-dried sample (0.5 wt%). Blue and red symbols indicate  $+1/2$  and  $-1/2$  disclinations, respectively. Reprinted with permission from (Angewandte Chemie International Edition **2011**, 50, (13), 3043–3047). Copyright (2011) John Wiley and Sons

### 1.3 Prospect of Inorganic Liquid Crystals

Considerable progress has been achieved in inorganic liquid crystals, however, more sophisticated understandings on this area are waiting to be explored in theory, experiments, engineering and applications. It is hard to prepare low dimensional inorganic particles (1D rod-like or 2D plate-like), which needs high temperature solid phase reaction. Dispersing/dissolving these inorganic particles in the solvents and preparing stable dispersion/solution is also difficult. For reasons above, only few kinds of inorganic liquid crystals were investigated. Compared with organic liquid crystals, inorganic liquid crystals are similar to rigid polymers and they are all unable to form thermotropic liquid crystals for high melting point, and thus only lyotropic liquid crystals can be achieved. In addition, the polymer dispersions are thermodynamic

stable systems, while inorganic liquid crystals are thermodynamic unstable for giant phase boundary. According to Gabriel and Davidson [2], surface charged colloidal particles are easier to form inorganic lyotropic liquid crystals. The reasons are listed as below: the surface charge will increase the stability of systems by reducing Van der Waals interaction between particles; The effective volume fraction of particles can be increased because of the double layer, and thus the phase transition concentration will be reduced; Plenty of counter-ions are released in the solution, increasing the system entropy and stability of liquid crystal.

## 2 The influence of gravity on inorganic lyotropic liquid crystals

Inorganic lyotropic liquid crystals are easy to be influenced by external fields, including gravity, electric field, magnetic field or confining geometries. As diameter of colloid particles are much larger than atoms ( $10^3$  to  $10^4$  times), and the interactions between particles are relatively weak. The gravity can obviously influence the phase behavior and dynamic of colloidal dispersion [36]. That is to say, gravity has significant influence on the formation of liquid crystals. At low concentration of colloidal dispersion, concentration gradient distributions are proportional to  $\exp(-z/l_g)$ , where  $z$  is vertical height, and  $l_g$  is gravitational length. For single particle, gravitational length can be used to the effect of gravity on phase behavior. As the Eq. (1) shows, gravitational length is inverse proportional to density difference and particle volume.

$$l_g = \frac{K_B T}{g \Delta \rho V_{\text{particle}}} \quad (1)$$

where  $g$  is gravitational acceleration,  $K_B T$  is thermodynamic energy. For example, if one particle has diameter of  $1 \mu\text{m}$ , the density difference to solvent ( $\Delta \rho$ ) is  $0.10 \text{ g mL}^{-1}$ , the gravitational length of diameter is about  $10 \mu\text{m}$ . The migration generated from gravity is 10 times larger than that from Brownian movement. For a polydisperse system, the chemical potential ( $K_B T$ ) of every components and every interface are all the same, and thus the components with different volume ( $V_{\text{particle}}$ ) have different gravitational length. For dispersions with higher concentration, different type of liquid phases coexists. The particle sediment and fractionation always coexist in colloidal dispersions, and thus rich phase behavior can be observed in settled dispersions.

## 2.1 Settlement and Fractionation in Inorganic Liquid Crystals Induced by Gravity

Vis et al. [37] observed nematic phase and lamellar phase at low volume fraction in silica coated gibbsite dispersions. The gravitational length of particles calculated by authors is far smaller than 1 mm, which is still large compared to the size of colloid particles. The particles will sediment rapidly under the gravity. The sedimentation of particles will significantly increase the concentration at the bottom of samples, thus facilitating the phase transition. The liquid crystal phase can be formed because of sedimentation, even in systems with low particle concentration. However, it is hard to obtain accurate volume fraction of liquid crystal phase transition.

Mourad et al. [38] succeeded in preparing columnar phase by 2  $\mu\text{m}$  diameter plate-like gibbsite particles. The SAXS results (Fig. 5) showed that upon going from the top toward the bottom of the sample the  $q$ -values of the intercolumnar reflections slightly increase, which indicate compaction of the structure and pointed toward the direct role of gravity. In addition, at low  $q$ -values up to four concentric Bragg reflections, the reflections are elliptical rather than round, and display elongations similar for all reflections. The “ $d$ ” value calculated by Bragg peak is smaller than that of ideal columnar phase. Furthermore, observation of texture under polarization microscopy shows the difference of fluctuations in the vertical direction compared to the horizontal direction, which implies the strong effect of gravitational compaction in the structure. The authors predicated that column undulations existed in the system and gravity-brought compaction has drastic influence on the system.

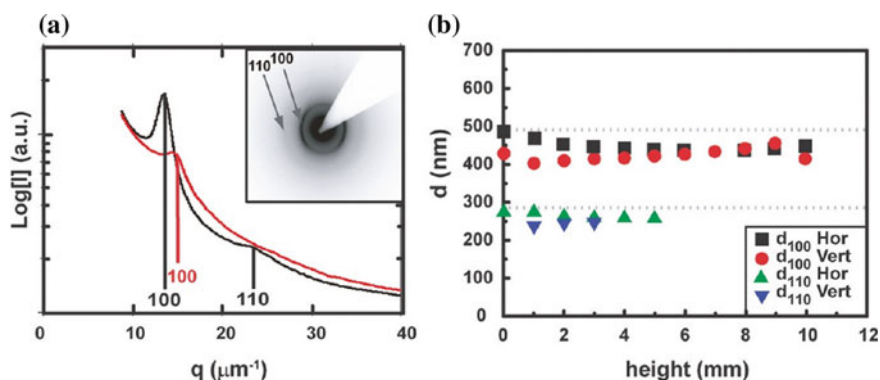


**Fig. 5** a Profiles of the X-ray scattering intensity in the horizontal (black curve) and vertical (red curve) direction of the concentrated sample. The inset shows the 2D high resolution SAXS pattern. b  $d_{100}$  and  $d_{110}$  recorded in the horizontal (Hor) and vertical (Vert) direction at different heights above the bottom of the sample. The dashed lines indicate the  $d_{100}$  ideal and  $d_{110}$  ideal assuming an intercolumnar distance based on the average diameter of the platelets (570 nm) and an ideal hexagonal lattice. Reprinted with permission from (Langmuir 2010, 26, (17), 14182–14187). Copyright (2010) American Chemical Society

Wijnhoven et al. [39] and Sun et al. [40] observed opposite phenomena on the competition between settlement, gelatinization and liquid phase transition of colloidal system (Fig. 6). The former found that the settlement took place prior to the liquid crystal phase transition, and thus sedimentations can be observed in the bottom of the cuvette. While the latter observed the settlement and liquid crystal phase behavior took place at the same time, and no sedimentations can be observed at the bottom of the cuvette. In order to explain the difference, both of them introduced Peclet number to describe the sedimentation/diffusion balance in gravitational field. Peclet number is the ratio of the time a particle takes to diffuse a distance equal to its diameter  $D$  to the time it takes to sediment this distance:  $P_e = t_{\text{diff}}/t_{\text{sed}} = (D^2/D')/(D/v_{\text{sed}})$ , where  $D'$  represents for the diffusion coefficient and  $v_{\text{sed}}$  the sedimentation velocity. Using the Einstein relation for infinite dilution  $D' = k_B T/f$  and  $v_{\text{sed}} = m^* g/f$ , with  $f$  the friction factor and  $m^*$  the particle buoyant mass,  $P_e = m^* g D/k_B T$ . As the gravitational length can be described as  $\xi = k_B T/m^* g$ ,  $P_e = D/\xi$ , which is a ratio of length scales. Increasing Peclet number lead to increased impact of gravity on particles. In fact, according to the results provided by both of the authors, the conformational transition can take place prior to the impact of gravity, that is to say, the settlement and liquid crystal phase transition should take place at the same time. The presence of sedimentation can be explained as: increasing particle concentration lead to higher probability of particle aggregation from Brownian movement. The aggregates increase the real diameter of particles and thus increasing the  $P_e$ . Sun et al. and Wijnhoven et al. observed similar phenomenon in high concentration systems.

van der Beek et al. [41, 42] investigated the influence of ionic strength and gravity on liquid crystal phase behavior of charged gibbsite systems. At relatively high ionic strength, the I–N phase transition was observed; at relatively low ionic strength, the I–C transition occurred. The experimental results are corresponding to the phase diagram obtained by Monte Carlo simulations [43]. After standing for 6 months under the gravitational field, a sample containing an isotropic and a nematic phase in coexistence (6:4) turns to three phases instead of I/N coexistence. The three phases are isotropic, nematic and columnar, from top to bottom, respectively. The particle concentration varied as a function of height, indicating a balance between gravity and osmotic pressure. The author used a simple model to describe this balance qualitatively.

An experimental study on gravity induced liquid crystal formation in gibbsite and silica mixed system was proposed by Kleshchanok et al. [44]. After one year of the sample preparation, all of pure gibbsite samples show coexisted I/N/C phase, which can be explained by gravity and sedimentation of platelets, leading to a density gradient in a capillary of sufficient height. However, for mixed gibbsite/sphere suspensions, the only observed liquid crystalline phase is a columnar phase, in coexistence with an isotropic phase (I/C), in contrast to nematic phase (N) of pure gibbsite systems. The authors ascribed this phenomenon to the strong depletion attraction in the mixture preventing the formation of gravity induced nematic phase. Adding silica sphere significantly broadened the I/C coexistence region.

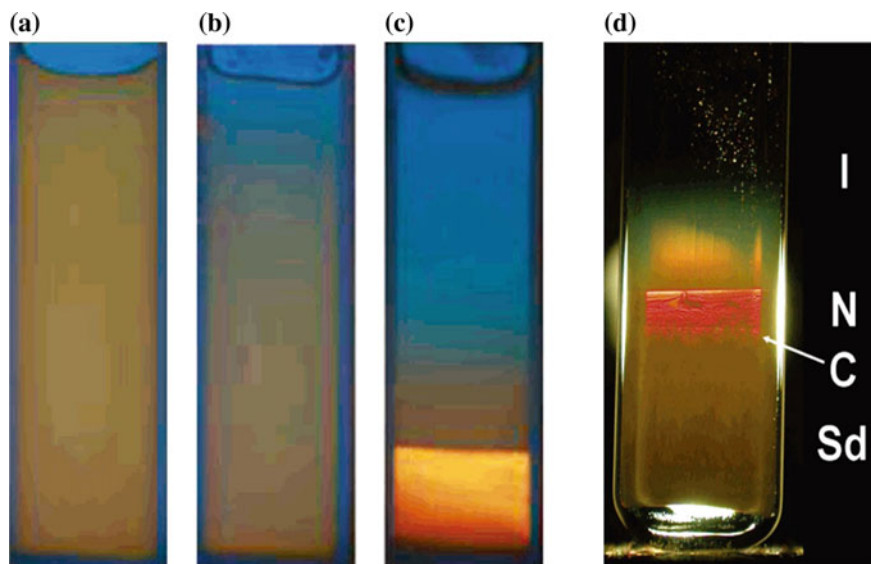


**Fig. 6** Phase behavior of 20% (w/w)  $Mg_2Al$  LDHs suspension as observed between crossed polarizers. **a** Right after preparation, **b** 39 days and **c** 8 months after preparation, **d** samples (Gibbsite platelets) at 1.5 year after preparation, and observed between crossed polarizers. An isotropic, nematic and columnar phase are visible together with an amorphous sediment. Reprinted with permission from (Langmuir **2007**, 23, (10), 5331–5337). Copyright (2007) American Chemical Society. Reprinted with permission from (Langmuir **2005**, 21, (23) 10422–10427). Copyright (2005) American Chemical Society

Zhang and van Duijneveldt [45] firstly used natural clay sepiolite particles to prepare nonaqueous (toluene) suspension. Clays were firstly treated with DODAB and then steric stabilizer SAP 230 (a poly isobutylene based stabilizer) was grafted onto the surface. In this suspension, isotropic-nematic phase separation can be observed at volume fraction above 0.06. A thin layer of a second birefringent nematic phase slowly forms on top of the initial nematic phase after samples standing for about 1 month, which can be considered as triphasic ( $I/N_1/N_2$ ) equilibrium. The gravitational field has great impact on the triphasic equilibrium of system, for the gravitational length  $\xi$  of particles is 0.64 mm and far smaller than the height of cuvette (20 mm). However, it is a pity that authors didn't give further explanation.

Dimasi et al. [46] presented synchrotron X-ray diffraction from gravity dispersed suspensions of Na fluorohectorite over a large NaCl concentration range. Two distinct gel regions were characterized by differences in orientational anisotropy and domain size. The polydispersity in particle size of Na fluorohectorite suspensions is also influenced by gravitational forces, which can sort the particles by size, stabilizing several strata of gels, sols and/or sediments within a single sample tube.

Sun et al. [47] investigated the phase behavior of  $Mg_2Al$  LDHs dispersions under microgravity, with the help of SJ-10 satellite. A series of equipments were designed

by Li et al. [48] to observe the lyotropic liquid crystals in situ on the satellite (Fig. 7a). The authors firstly performed a pilot study of the liquid crystal phase transition in polydisperse  $\text{Mg}_2\text{Al}$  LDHs under normal gravity. The dispersions are isotropic under the polarizer observation at low concentration ( $<23$  wt%) (Fig. 7c). With increasing concentration (23–30 wt%) of  $\text{Mg}_2\text{Al}$  LDHs, the dispersions show a shear-induced birefringence, indicating a highly-ordered directional alignment of particles. Coexistence of four phases, including an opaque isotropic top phase, a birefringent middle phase, a faint birefringence new phase and a sediment layer of larger platelets, are observed after standing for 5 days (Fig. 7d). When concentration increased up to 32 wt%, three phases coexistence (I/N/S) are observed (Fig. 7e). The authors chose five samples with concentration from 22 to 30 wt% to perform microgravity experiments. The liquid crystal phase transition of  $\text{Mg}_2\text{Al}$  LDHs under microgravity is observed and indicates that the Onsager's theory remained valid under microgravity (Fig. 7f, g). The phase transition concentration increased from 25 wt% under normal gravity to 27 wt% under microgravity, which proves the gravity-brought fractionation facilitate the liquid crystal transition. In addition, relax time of shear-induced birefringence is significantly increased under microgravity, which can be explained by low Peclet number of the  $\text{Mg}_2\text{Al}$  LDHs particles.

## 2.2 Weakened Impact of Polydispersity in Gravitational Field

In contrast to highly monodisperse rod-like virus [49], the natural or synthetic inorganic colloidal particles are commonly polydisperse [50]. The polydispersity inhibit the formation of ordered structures [51]. However, in the gravitational field, the inhibition of polydispersity on liquid crystal phase transition will be weakened for the fractionation. Vroege et al. [52] observed smectic phase in dispersions of highly polydisperse rod-like goethite nanoparticles. However, Monte carlo simulation showed a terminal polydispersity ( $s > 0.18$ ), above which the smectic phase will be no longer stable [53]. The authors predicted that in gravitational field, particles fractionation induced by gravity will significantly reduce the polydispersity, and thus facilitating the formation of smectic phase. Two systems with  $\sigma_D = 0.55$  and  $\sigma_D = 0.17$  ( $\sigma_D$ : polydispersity) was investigated. For  $\sigma_D = 0.55$ , smectic phase and columnar phase in systems are observed, while for  $\sigma_D = 0.17$  no columnar phase could be observed in systems. The average length drastically increased to the bottom of the capillary indicating fractionation during sedimentation. Polydispersity is the lowest in the part where only a smectic phase occurred. In contrast, The part where smectic phase coexisted with columnar phase has higher polydispersity, consistent with the notion that the columnar phase can accommodate particles that do not fit into the smectic layers.

For nematic phase, long particles with high excluded volume will be preferred orientation. This tendency will be enhanced because of the sedimentation and lead to extra fractionation. The internal polydispersity of inorganic particles will inhibit the formation of spatial ordered structure (smectic phase or columnar phase). Rod-like particles with low dispersibility will form smectic phase. For particles with

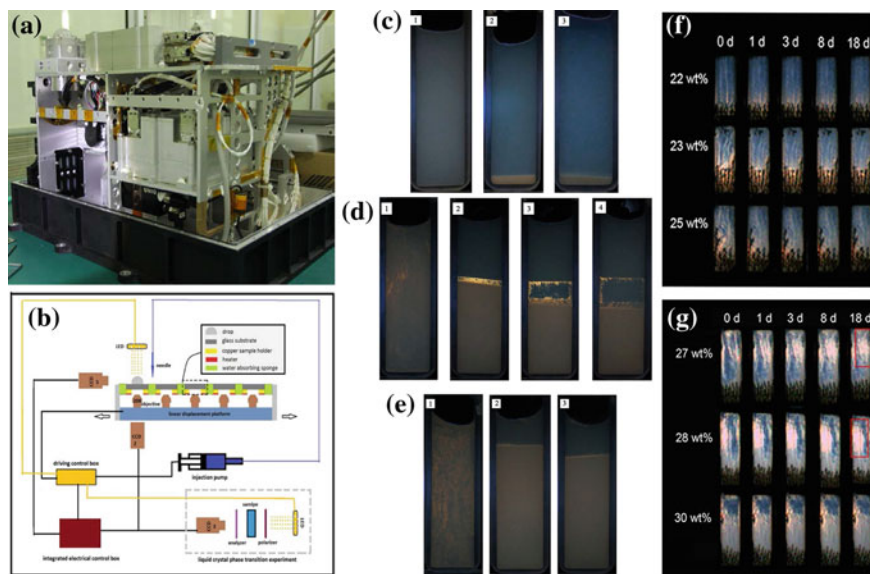


**Fig. 7** **a** The internal structure of the colloidal material box. **b** Experimental principle diagram of the colloidal material box. Reprinted figure with permission from [Microgravity Science and Technology **2016**, 28, (2), 179–188]. Copyright (2016) by the Springer. **c** Polarized light photographs of the 16 wt% Mg<sub>2</sub>Al LDHs suspension: (1) just prepared, (2) 5 days, (3) 15 days. **d** Polarized light photographs of the 28 wt% Mg<sub>2</sub>Al LDHs suspension: (1) just prepared, (2) 5 days, (3) 12 days, (4) 15 days. Reprinted figure with permission from [Microgravity Science and Technology **2016**, 28, (2), 95–100]. Copyright (2016) by the Springer. **e** Polarized light photographs of the 32 wt% Mg<sub>2</sub>Al LDHs suspension: (1) just prepared, (2) 12 days, (3) 15 days. **f** and **g** Polarized optical micrographs of the phase behavior of different concentration samples under microgravity at different time. “0 d” represents “immediately after magnetic stirring”. The bead-shaped spheres in the bottom of cuvette are nickel powder fixed by a magnet

higher dispersibility, they tend to form nematic phase rather than unstable smectic phase at lower concentration, or form columnar phase at higher concentration [54]. For example, In systems of plate-like gibbsite particles, the formation of columnar phase is very slow [41]. However, the formation process can be accelerated under a centrifugation force of 900 *g* without arresting the system in a disordered glassy phase, and numerous small crystallites were also observed [55] (Fig. 8).

Petukhov et al. [56] observed of one type of columnar liquid crystal phase formed by thin hard colloidal disks in a dense suspension. The combination of long-range bond-orientational order and short-range translational order between the columns is explained for the size polydispersity of the particles. As Fig. 9 shows, three-phase equilibrium of the isotropic, nematic, and columnar phases is observed between crossed polarizers (Fig. 9a). The columnar phase can be identified by strong Bragg reflections of visible light (Fig. 9c, d). The hexaticlike columnar phase formation is ascribed for the colloidal disks’ accommodation of polydispersity at high compression. Close to the N/C transition, the system forms a powder consisting of true

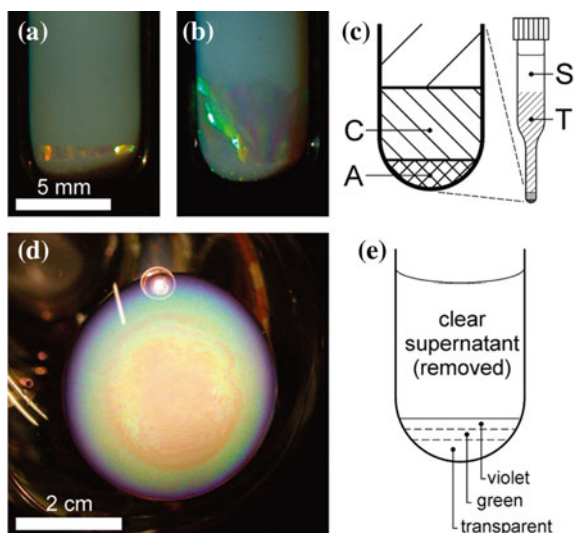


**Fig. 8** **a** and **b** Iridescent columnar phase grown in a gravitational field. Samples have been standing for 2 and 4 years, respectively, at 1g. The scale bar pertains to both images. **c** Sketch of the crystallization tube and its layers: S is the clear supernatant, T is the turbid suspension, C is the well-ordered columnar crystalline layer, and A is the amorphous columnar crystal. **d** At 900g, using a centrifuge, it takes only 1 day to create a columnar phase. **e** Sketched layers of the sample. Reprinted with permission from (Langmuir **2007**, 23, (23), 11343–11346). Copyright (2007) American Chemical Society

long-range-ordered columnar crystallites, where the relatively large free space between the columns allows for the accommodation of rather highly polydisperse particles. However, for lower ones, due to gravitational compression, little space is available. The geometrical frustration induced by the particle polydispersity suppresses the ordering upon increasing density and favor hexaticlike structuring.

One method to reduce polydispersity of colloidal plates by the synergistic effect of self assembly and gravity was brought by Cheng et al. [57]. The samples were prepared by diluting a concentrated ZrP suspension with deionized water and I/N separation occurred after 5 days. The lower N phase and upper I phases were extracted separately to reduce the polydispersity of the particles. The nematic phases were collected repeatedly for use in the subsequent fractionation. At the concentration of 1.07 wt%, the polydispersity can be reduced from 0.27 to 0.17. This polydispersity reduction method based on the I/N phase transition and gravity can be utilized to select nanoplates with a certain size and to improve size monodispersity.

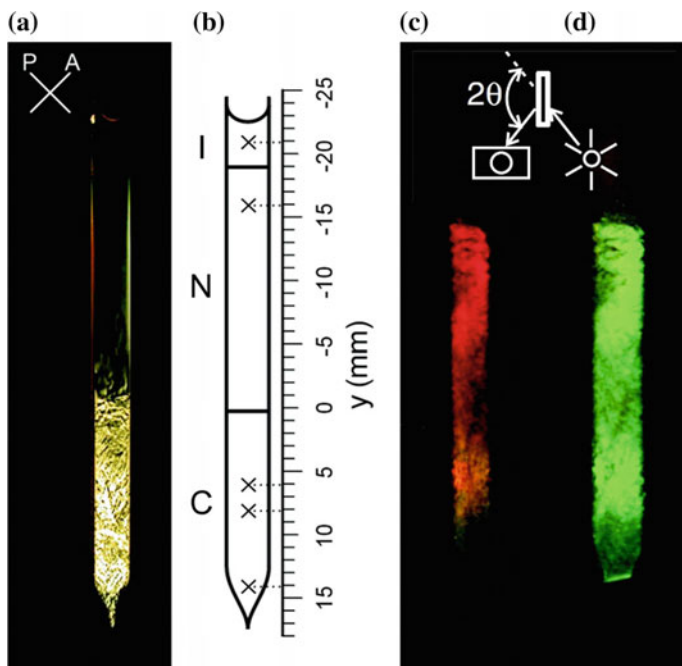


**Fig. 9** **a** Depicts the sample between crossed polarizers (orientation is indicated in the left top) and panel. **b** Identifies the isotropic, nematic, and columnar phase. Crossed mark the positions in the sample where SAXS patterns were taken. **c** and **d** Close-ups of the columnar phase, capturing the Bragg reflections at two different Bragg angles of  $2\theta = 140^\circ$  (**c**) and  $2\theta = 120^\circ$  (**d**). Reprinted with permission from (Physical Review Letters **2005**, 95, 077801). Copyright (2005) American Physical Society

### 3 Conclusion

For the large size and weak particle–particle interactions, gravity can significantly influence the phase behavior of inorganic colloidal particles and further influence the liquid crystal phase transition. The phase behavior of liquid crystals without external forces can only be observed under microgravity, which was rarely reported. Gravity-induced fractionation can be observed in liquid crystals systems, which can obviously reduce the impact of polydispersity on the liquid crystal transition. The polydispersity of original dispersion cannot be maintained after standing for long time for gravity. It is necessary to avoid the impact of gravity during the investigation in polydispersity and liquid crystals transition. To provide a microgravity situation, perform the experiments in satellite or space station will be effective, and thus results can be compared to the corresponding ones on earth to understand the impact of gravity. In brief, inorganic liquid crystal transition under microgravity is a promising research aspect in future.

## References

1. Steffen W, Köhler B, Altmann M, Scherf U, Stitzer K, zur Loye HC, Bunz UH (2001) *Chem-A Eur J* 7:117
2. Gabriel JC, Davidson P (2000) *Adv Mater* 12:9
3. Freundlich H (1916) *Zeitschrift für Elektrochemie und angewandte physikalische Chemie* 22:27
4. Zocher H (1921) *Z Phys Chem* 98:293
5. Zocher H, Török C (1967) *Acta Crystallogr A* 22:751
6. Langmuir I (1938) *J Chem Phys* 6:873
7. Pelletier O, Bourgaux C, Diat O, Davidson P, Livage J (1999) *Eur Phys J B-Condens Matter Complex Syst* 12:541
8. Pelletier O, Davidson P, Bourgaux C, Coulon C, Regnault S, Livage J (2000) *Langmuir* 16:5295
9. Davidson P, Bourgaux C, Schouffet L, Sergot P, Williams C, Livage J (1995) *J Phys II* 5:1577
10. Comminhes X, Davidson P, Bourgaux C, Livage J (1997) *Adv Mater* 9:900
11. Lamarque-Forget S, Pelletier O, Dozov I, Davidson P, Martinot-Lagarde P, Livage J (2000) *Adv Mater* 12:1267
12. Desvaux H, Gabriel JCP, Berthault P, Camerel F (2001) *Angew Chem Int Ed* 40:373
13. Camerel F, Gabriel JC, Batail P (2003) *Adv Func Mater* 13:377
14. Buining P, Philipse A, Lekkerkerker H (1994) *Langmuir* 10:2106
15. Buining P, Veldhuizen Y, Pathmamanoharan C, Lekkerkerker H (1992) *Colloids Surf* 64:47
16. Lemaire B, Davidson P, Ferré J, Jamet J, Panine P, Dozov I, Jolivet J (2002) *Phys Rev Lett* 88:125507
17. Zocher H, Birstein V (1929) *Z Phys Chem* 141:413
18. Maeda H, Maeda Y (1996) *Langmuir* 12:1446
19. Emerson W (1956) *Nature* 178:1248
20. Mouchid A, Delville A, Lambard J, Lecolier E, Levitz P (1995) *Langmuir* 11:1942
21. Gabriel JP, Sanchez C, Davidson P (1996) *J Phys Chem* 100:11139
22. Levitz P, Lecolier E, Mouchid A, Delville A, Lyonard S (2000) *EPL (Eur Lett)* 49:672
23. van der Kooij FM, Kassapidou K, Lekkerkerker HN (2000) *Nature* 406:868
24. Van der Beek D, Lekkerkerker H (2003) *EPL (Eur Lett)* 61:702
25. Rives V (2001) *Layered double hydroxides: present and future*. Nova Publishers
26. Constantino VR, Pinnavaia TJ (1995) *Inorg Chem* 34:883
27. Stupp SI, Braun PV (1997) *Science* 277:1242
28. Liu S, Zhang J, Wang N, Liu W, Zhang C, Sun D (2003) *Chem Mater* 15:3240
29. Xu Z, Gao C (2011) *Nature communications* 2:571
30. Kim JE, Han TH, Lee SH, Kim JY, Ahn CW, Yun JM, Kim SO (2011) *Angew Chem Int Ed* 50:3043
31. Dan B, Behabtu N, Martinez A, Evans JS, Kosynkin DV, Tour JM, Pasquali M, Smalyukh II (2011) *Soft Matter* 7:11154
32. Kim J, Cote LJ, Kim F, Yuan W, Shull KR, Huang J (2010) *J Am Chem Soc* 132:8180
33. Zamora-Ledeza C, Puech N, Zakri C, Grelet E, Moulton SE, Wallace GG, Gambhir S, Blanc C, Anglaret E, Poulin P (2012) *J Phys Chem Lett* 3:2425
34. Kou L, Gao C (2013) *Nanoscale* 5:4370
35. Hu X, Xu Z, Gao C (2012) *Sci Rep* 2:767
36. Royall C, van Roij R, Van Blaaderen A (2005) *J Phys: Condens Matter* 17:2315
37. Vis M, Wensink H, Lekkerkerker H, Kleshchanok D (2015) *Mol Phys* 113:1053
38. Mourad MC, Petukhov AV, Vroege GJ, Lekkerkerker HN (2010) *Langmuir* 26:14182
39. Wijnhoven JE, van't Zand DD, van der Beek D, Lekkerkerker HN (2005) *Langmuir* 21:10422
40. Zhang J, Luan L, Zhu W, Liu S, Sun D (2007) *Langmuir* 23:5331
41. van der Beek D, Schilling T, Lekkerkerker HN (2004) *J Chem Phys* 121:5423
42. van der Beek D, Lekkerkerker HN (2004) *Langmuir* 20:8582
43. Veerman J, Frenkel D (1992) *Phys Rev A* 45:5632

44. Kleshchanok D, Meijer J-M, Petukhov AV, Portale G, Lekkerkerker HN (2012) *Soft Matter* 8:191
45. Zhang Z, van Duijneveldt JS (2006) *J Chem Phys* 124:154910
46. Dimasi E, Fossum JO, Gog T, Venkataraman C (2001) *Phys Rev E* 64:061704
47. Chen Y, Zhang L, Sun D, Sun Z, Xu S (2016) *Microgravity Sci Technol* 28:95
48. Li W, Lan D, Sun Z, Geng B, Wang X, Tian W, Zhai G, Wang Y (2016) *Microgravity Sci Technol* 28:179
49. Lettinga MP, Kang K, Holmqvist P, Imhof A, Derks D, Dhont JK (2006) *Phys Rev E* 73:011412
50. Palberg T (2014) *J Phys: Condens Matter* 26:333101
51. Vroege GJ, Thies-Weesie DM, Petukhov AV, Lemaire BJ, Davidson P (2006) *Adv Mater* 18:2565
52. Van den Pol E, Thies-Weesie D, Petukhov A, Vroege G, Kvashnina K (2008) *J Chem Phys* 129:164715
53. Bates MA, Frenkel D (1998) *J Chem Phys* 109:6193
54. Sun D, Sue H-J, Cheng Z, Martínez-Ratón Y, Velasco E (2009) *Phys Rev E* 80:041704
55. van der Beek D, Radstake PB, Petukhov AV, Lekkerkerker HN (2007) *Langmuir* 23:11343
56. Petukhov AV, van der Beek D, Dullens RPA, Dolbnya IP, Vroege GJ, Lekkerkerker HN (2005) *Phys Rev Lett* 95:077801
57. Chen F, Chen M, Chang Y, Lin P, Chen Y, Cheng Z (2017) *Soft Matter* 13:3789